Astron. Astrophys. 317, 752–760 (1997)

ASTRONOMY
AND
ASTROPHYSICS

Ducted fast waves in coronal loops: curvature effects

J.M. Smith[1], **B. Roberts**[1], **and R. Oliver**[2]

[1] School of Mathematical and Computational Sciences, University of St Andrews, North Haugh, St Andrews, Fife KY16 9SS, Scotland.
[2] Departament de Física, Universitat de les Illes Balears, E-07071 Palma de Mallorca, Spain

Received 23 April 1996 / Accepted 11 June 1996

Abstract. We examine the effect of curvature on fast magnetoacoustic waves in dense coronal loops situated in a potential coronal arcade. The wave equation governing the velocity perturbations has been solved numerically under the zero-β approximation and in the absence of gravity. Due to the curvature of the structure, leaky waves arise. The extent of the leakage depends upon the length, width and density enhancement of the loop, as well as the frequency of oscillation and its geometrical nature. The sausage mode is more affected by curvature and is more leaky than the kink mode. An increase in length, width or gas density ratio reduces the leakage, whilst higher frequencies result in greater energy leakage. Odd modes of oscillation (zero velocity at the loop summit) are more strongly confined than even modes. Modes of oscillation may be destroyed by curvature and above a critical frequency ducted waves cease to exist.

Key words: MHD – Sun: corona – Sun: magnetic field – Sun: oscillations

1. Introduction

Recent observations of X-ray emission from the solar corona by Yohkoh (Shibata et al. 1992; Acton et al. 1992) have emphasised the complex, highly structured nature of the corona. The active region corona consists mainly of dense loops, the transverse dimensions of which are much shorter than the longitudinal ones (Golub 1991). Understanding the physical nature of wave propagation in such structures offers potentially important seismic information about the corona. The gas density in active region loops is approximately a factor 3 to 10 times greater than the surrounding plasma. Foukal (1975) gives a density enhancement of 4 whilst Stewart (1976), using a coronal density model derived from radio observations of active regions, found a density enhancement of 8 to 10. Pick et al. (1979), analysing a coronal structure, found the density to be 10 times higher than the surrounding plasma. Cheng (1980) reports a low gas density ratio between a loop and the surrounding corona of 7/5. Observations from Yohkoh suggest the density contrast between the inside and outside of loops is a factor greater than 10 (Tsuneta 1996). However, in flare loops, the gas density can be 100 times higher than the neighbouring plasma (Aschwanden 1994), with the highest densities occurring at the loop summit (Doschek et al. 1995). A comprehensive review of observations of coronal loops is given by Bray et al. (1991).

Observations suggest that periodic and quasi-periodic oscillations commonly occur in the corona. Oscillations are detected by measuring the temporal variation in intensity, line width and Doppler velocity of coronal emission lines and are summarised, together with prominence oscillations, by Tsubaki (1988). Many of the observed periods are of the order of five minutes, although Pasachoff & Landman (1984) and Pasachoff & Ladd (1987) detected intensity variations of the green coronal line with periods of 0.5 to 4 seconds. Koutchmy (1981) used Doppler velocity measurements of the green coronal line and reported oscillations of 43, 80 and 300 seconds. Further information about oscillations of the coronal plasma comes from radio and X-ray emission, with periods ranging from sub-second to several minutes. Short, one second, periods of oscillation are abundantly reported (e.g. Trottet et al. 1981; Zodi & Kaufmann 1984; Wiehl et al. 1985; Zhao et al. 1990). Periods longer than 60 seconds have been reported by Trottet et al. (1979). Various theoretical models have been proposed to explain these observations and are reviewed in Aschwanden (1987).

The ducted wave model of Roberts et al. (1983, 1984) suggests that dense coronal loops act as waveguides with fast magnetoacoustic waves trapped in regions of high density (low Alfvén speed). To gain physical insight the coronal loop was modelled as a dense slab or cylinder embedded in a uniform magnetic field (Edwin & Roberts 1982, 1983). Two modes were extensively studied, the symmetric (*sausage*) mode and the asymmetric (*kink*) mode. The symmetric oscillations have an analogy in oceanography (Pekeris waves), whilst asymmetric disturbances are related to the Love waves of seismology. In the sausage mode, the magnetic slab or cylinder pulsates like a blood vessel, with its central axis remaining undisturbed. In the kink mode, the central axis moves back and forth during the wave motion.

Send offprint requests to: J.M. Smith

The fast mode velocity can have nodes in the two spatial directions, along the loop length and across the loop width. In the case of nodes across the loop, kink and sausage modes with the least number of nodes are referred to as *principal* modes. Traversing the slab or cylinder from one boundary to the other, the velocity in the principal kink mode does not change sign and the velocity in the principal sausage mode changes sign once only, on the central axis. The *overtones* of the principal kink and sausage mode have a greater number of oscillations in the direction perpendicular to the axis.

In a zero-β magnetic slab, the principal sausage mode occurs only for wavenumbers k above a critical cutoff, k^{crit}, given by (Roberts et al. 1983)

$$k^{crit} = \frac{\pi}{2a}\left(\frac{v_{A0}^2}{v_{Ae}^2 - v_{A0}^2}\right)^{\frac{1}{2}} , \tag{1}$$

where $2a$ is the width of the slab and v_{A0} and v_{Ae} ($> v_{A0}$) are the Alfvén speeds inside and outside the slab respectively. By contrast, the principal kink mode occurs for all k, although its overtones have wavenumber cutoffs. Consequently, the sausage mode has a shorter period than the kink. The period of oscillation at the onset of the sausage mode can be estimated by

$$\tau_{saus} = \frac{4a}{v_{A0}}\left(1 - \frac{v_{A0}^2}{v_{Ae}^2}\right)^{\frac{1}{2}} . \tag{2}$$

Roberts et al. (1983, 1984) found that under typical coronal conditions the periods of the sausage and kink modes are 1–2 seconds and 40–60 seconds respectively, in good agreement with observations.

We extend this model by considering the more realistic situation of ducted waves in curved loops in a potential coronal arcade. The wave equation is solved numerically using a finite difference code developed by Oliver, Hood & Priest (1996). The code solves two coupled partial differential equations with non-constant coefficients in generalised coordinates. By analogy with the work on bounded waves in curved waveguides (e.g. Gloge 1972), we may expect leaky waves to arise in curved loops (Edwin 1984).

Roberts et al. (1983, 1984) considered solely evanescent modes in the exterior of the loop. For such modes, in a zero-β plasma, the effective transverse wavenumber for a wave of frequency ω and longitudinal wavenumber k is $m_e = \left(k^2 - \omega^2/v_{Ae}^2\right)^{\frac{1}{2}}$. Modes that are evanescent in the environment of a slab (or tube) are such that $\omega^2 < k^2 v_{Ae}^2$, for which m_e is real and positive; no energy leakage from the slab occurs. It is possible also for disturbances to arise that *leak* into the environment; for such modes m_e^2 is no longer positive. Such modes have been considered by Meerson, Sasorov and Stepanov (1978), Roberts & Webb (1979), Wilson (1981) and Spruit (1982), supposing the frequency ω to be complex (so that waves are now only partly guided by the loop, with wave energy being lost from the loop). Cally (1986) investigates leakage from cylindrical flux tubes comprehensively. Čadež & Okretič (1989) examine surface wave leakage also through the use of complex frequency. Davila (1985) examined leaky waves in a coronal hole modelled in a slab geometry; the structure was found to act as a leaky waveguide. Finally, Murawski & Roberts (1993) studied numerically wave leakage from a coronal loop modelled as a smoothed slab embedded in a uniform magnetic field. The leakage in this case arose in a spatially smooth density profile. In this work we study the leakage from loops arising because of the curved geometry of an arcade.

2. Wave propagation in an arcade

2.1. The wave equation

We consider a two-dimensional (x, z) coronal arcade which is invariant in the $y-$direction, modelled as a potential magnetic field satisfying

$$\nabla \times \mathbf{B} = \mathbf{0} . \tag{3}$$

From the solenoidal constraint $\nabla \cdot \mathbf{B} = 0$, the equilibrium magnetic field $\mathbf{B}$ can be written as

$$\mathbf{B} = \nabla A(x,z) \times \hat{\mathbf{e}}_y = \left(-\frac{\partial A}{\partial z}, 0, \frac{\partial A}{\partial x}\right) , \tag{4}$$

where the magnetic flux function $A(x,z)$ satisfies $\nabla^2 A = 0$. The solution for A is obtained by separation of variables, with the condition that A is zero at infinite height and the $z-$component of the magnetic field is zero at the centre of the arcade. In this configuration, the field lines are aligned with the z-axis at $x = \pm L$, with $2L$ being the width of the arcade. The flux function, which is constant along a field line, is given by

$$A(x,z) = B_0 \Lambda_B \cos\left(\frac{x}{\Lambda_B}\right) \exp\left(-\frac{z}{\Lambda_B}\right) , \tag{5}$$

where B_0 is the magnetic field strength at the base ($z = 0$) of the corona and $\Lambda_B = 2L/\pi$ is the magnetic scale height. The field components are

$$\begin{aligned} B_x &= B_0 \cos\left(\tfrac{x}{\Lambda_B}\right) \exp\left(-\tfrac{z}{\Lambda_B}\right) , \\ B_z &= -B_0 \sin\left(\tfrac{x}{\Lambda_B}\right) \exp\left(-\tfrac{z}{\Lambda_B}\right) . \end{aligned} \tag{6}$$

The form of the potential coronal arcade is shown in Fig. 1.

Consider the linearised equations of magnetohydrodynamics (MHD) assuming that the plasma-β is zero (cold plasma) and gravity is negligible. The wave equation for plasma motions $\mathbf{v}$ is

$$\rho_0(x,z)\,\frac{\partial^2 \mathbf{v}}{\partial t^2} = \frac{1}{\mu_0}\left\{\nabla \times [\nabla \times (\mathbf{v} \times \mathbf{B})]\right\} \times \mathbf{B} , \tag{7}$$

with $\rho_0(x,z)$ the equilibrium gas density. Eq. (7) governs the velocity perturbations of the fast and Alfvén modes. In the zero-β approximation (the corona is magnetically dominated) there are no motions along the equilibrium magnetic field $\mathbf{B}$ because the only driving force is the $\mathbf{j} \times \mathbf{B}$ force, and the slow mode is absent because we have set the gas pressure to zero. We ignore

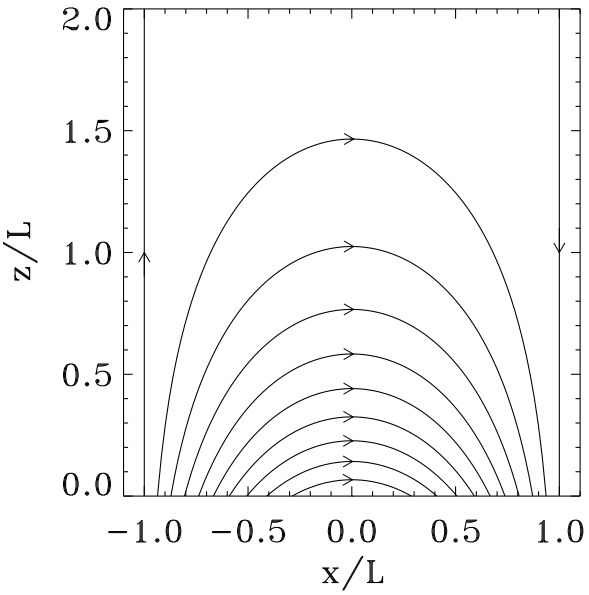

Fig. 1. The form of the potential arcade in Cartesian coordinates (x, z). The arcade is physically isolated from its surroundings by vertical planes located at $x = \pm L$

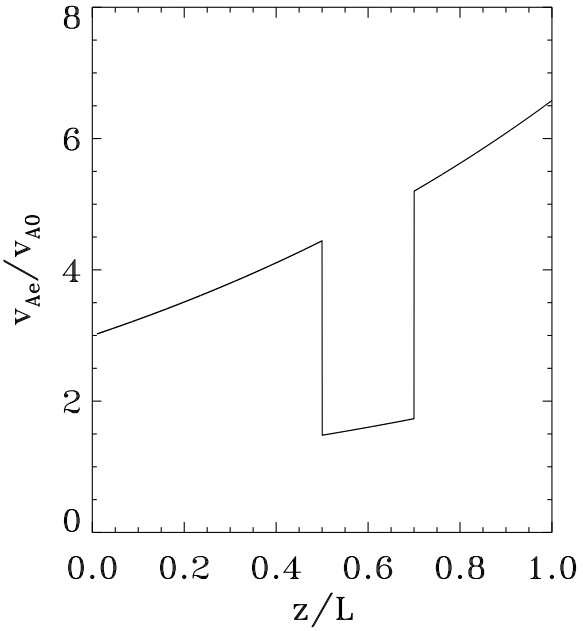

Fig. 2. The Alfvén speed profile v_A $(x = 0, z)$ for $\rho \left(= v_{Ae}^2/v_{A0}^2\right) = 9$. The dense loop (corresponding to a depression in Alfvén speed) is situated between $z/L = 0.5$ and $z/L = 0.7$

the Alfvén mode by setting $v_y = B_y = 0$ so only v_n, the velocity component normal to **B**, remains. Then, for motions of frequency ω, Eq. (7) reduces to

$$\nabla^2 (Bv_n) + \frac{\omega^2}{v_A^2} Bv_n = 0 \ , \tag{8}$$

where $B = B_0 \exp\left(-z/\Lambda_B\right)$.

Since we are neglecting the pressure and gravity terms in the momentum equation we are able to impose the density or Alfvén speed profile arbitrarily. From the analytical work by Roberts et al. (1983, 1984) it is known that ducted waves occur in regions of low Alfvén speed (high density). A loop is thus modelled as a region contained between two field lines in which a depression in the Alfvén speed occurs. However, special care must be taken when defining v_A. Oliver et al. (1993) investigated the normal modes of oscillation of the present magnetic structure for a variety of density profiles and found that whenever the Alfvén speed decreases or remains constant with height the solutions for v_n diverge as z tends to infinity. We find this property undesirable because it makes the interpretation of the results difficult. We thus choose a v_A (x, z) that exponentially increases with height z inside and outside the coronal loop, taking

$$v_A = \begin{cases} v_{A0} \exp\left(\frac{z}{2\Lambda_B}\right), & A_2 \leq A \leq A_1 \ , \\ v_{Ae} \exp\left(\frac{z}{2\Lambda_B}\right), & \text{otherwise} \ . \end{cases} \tag{9}$$

Here A_1 and A_2 $(< A_1)$ are chosen values of the flux function.

We introduce the parameter $\rho = v_{Ae}^2/v_{A0}^2$, which gives the density enhancement of the loop compared to the surrounding plasma; ρ must be greater than unity in order to have ducted waves in the loop. The Alfvén speed profile for $\rho = 9$ is shown in Fig. 2. Outside the dense loop the Alfvén speed increases exponentially, thus ensuring a rapidly decreasing velocity for waves outside the loop (Oliver et al. 1993). With this profile any increasing velocity outside the loop must originate from the loop and thus is a signature of leaky waves.

2.2. Numerical code and boundary conditions

The numerical code we employ was developed by Oliver et al. (1996) to solve the fast and slow mode equations in a two-dimensional equilibrium with no gravity. Oliver et al. cast these equations as two coupled partial differential equations, with non-constant coefficients, in which the velocity components normal and parallel to the equilibrium magnetic field (v_n and $v_\parallel$) are the unknowns. The equations were discretised using a finite difference scheme and the resulting algebraic eigenproblem was solved by inverse vector iteration, yielding individual eigenvalues, ω_d^2, together with v_n on a rectangular grid of points. The eigenvalue ω_d^2 is the dimensionless frequency squared: $\omega_d^2 \equiv \left(\omega L/v_{A0}\right)^2$. The eigenvalue takes real values only, so any energy leakage observed is attributable to the magnetic geometry. Extensive checks on the accuracy of the code have been made, including a comparison with the analytical work of Roberts et al. (1983, 1984) for a straight slab. Excellent agreement has been found. In all numerical computations we use 60×60 points in our simulation region.

The code provides the capability of modifying the coordinate system, using a pair of generalised coordinates. For example, these coordinates can be the Cartesian coordinates (x, z), with $-1 \leq x/L \leq 1$ and $0 \leq z/L \leq H$. The main drawback of this coordinate system is that it is not possible to consider the full height of the arcade, although one suspects that ducted modes,

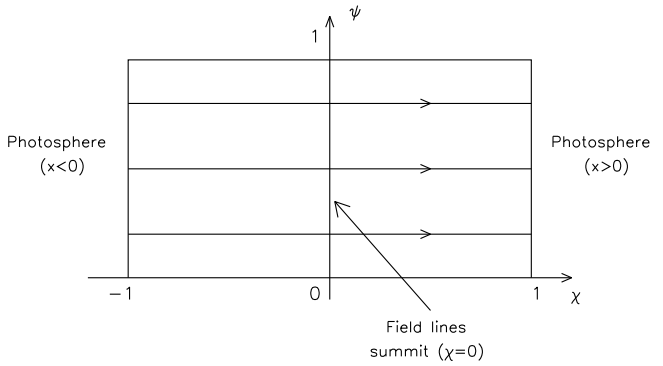

Fig. 3. A potential coronal arcade in flux coordinates (χ, ψ). Field lines are horizontal, given by $\psi = constant$. The photosphere is modelled by $\chi = -1\,(x < 0)$ and $\chi = 1\,(x > 0)$. All field lines have length 2

with exponentially decreasing velocity amplitudes outside the loop, will be obtained with good precision using a reasonable value of H. However, in order to investigate the effects of curvature it is convenient to use a flux coordinate system covering the whole arcade (Oliver et al. 1996). In the (χ, ψ) coordinates the curved loop in Cartesians becomes horizontal. The flux coordinates are given by

$$\begin{aligned} \psi &= \cos\left(\tfrac{x}{\Lambda_B}\right)\exp\left(-\tfrac{z}{\Lambda_B}\right)\ , \\ \chi &= \left(1-\psi^2\right)^{-\frac{1}{2}}\sin\left(\tfrac{x}{\Lambda_B}\right)\exp\left(-\tfrac{z}{\Lambda_B}\right)\ , \end{aligned} \tag{10}$$

with $0 \le \psi \le 1$ and $-1 \le \chi \le 1$. Note that ψ is proportional to the flux function, A. The potential arcade illustrated in Fig. 1 in Cartesians is shown again in Fig. 3 in flux coordinates. Field lines are now horizontal, given by ψ =constant. The field lines in the (χ, ψ) system all have length 2, which is achieved through the normalisation factor $\left(1-\psi^2\right)^{-\frac{1}{2}}$ in Eq. (10).

The line $\psi = 0$ is the field line in the (x, z) system that originates at $(-L, 0)$, extending up to infinity, and terminating at $(L, 0)$. The photosphere is modelled by $\chi = -1\,(x < 0)$ and $\chi = 1\,(x > 0)$. The line $\psi = 1$ is the point $x = z = 0$. We have assumed that the velocity **v** vanishes at the coronal base $z = 0$ ($\chi = \pm 1$ and $\psi = 1$), modelling the line-tying boundary condition at the photosphere (see, for example, Van der Linden, Hood & Goedbloed 1994). The arcade under consideration is taken to be isolated in the sense that no plasma traverses the boundaries at $x = \pm L$ ($\psi = 0$). The trapped waves are unaffected by the boundary condition imposed at $\psi = 0$. However, the behaviour of the leaky waves is influenced by the rigid wall. Taking the velocity, v_n, to be zero at $\pm L$ means any leaky waves are contained in the arcade. Leaky waves will therefore oscillate in a similar manner to the modes studied by Oliver et al (1993). Of course, in practice, no rigid walls exist at the edges of the arcade. Therefore, we may expect these waves to propagate away from the loop and to be observable at large heights in the corona. In the optical waveguide context, Snyder and Love (1983) suggest that a varying degree of leakage along a waveguide results in a similar spatial variation of velocity perpendicular to the guide (at a fixed location along the waveguide).

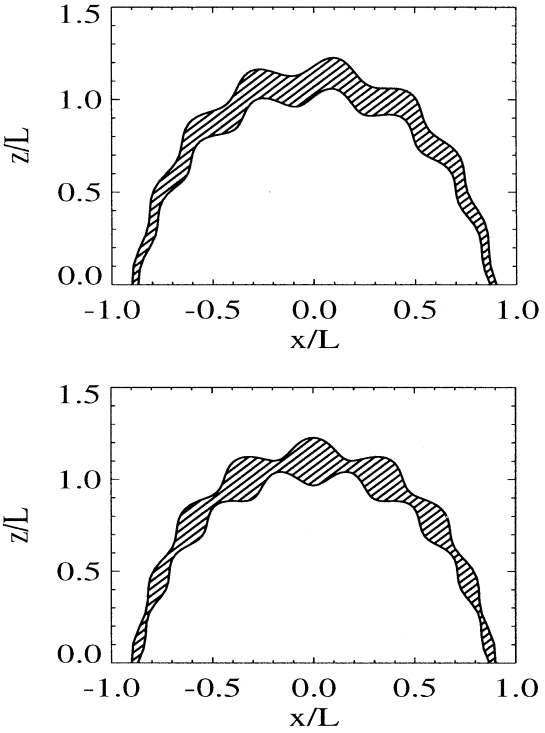

Fig. 4a and b. Schematic diagram of the fast mode velocity field associated with (**a**) a kink mode and (**b**) a sausage mode in a curved geometry. The spatial distribution of velocities needs to be multiplied by a term of the form $\cos \omega t$ to obtain the full temporal evolution. Kink modes give rise to lateral displacements of the loop about its central axis, while sausage modes are characterised by leaving the loop's axis undisturbed and producing converging and diverging plasma motions about the axis

To examine the effects of curvature we focus attention on different loops within our arcade. These loops have different lengths and hence the effect of curvature in each loop is different. For "long" loops, the length is much greater than the horizontal distance between its footpoints, whereas for "short" loops the length of the loop is comparable to the distance between its footpoints. Curvature effects are expected to be more important in short loops. Taking $L = 1.5 \times 10^5$ km gives the distance between the footpoints of the loops considered to be of the order 2×10^5 km. In addition, we take $v_{A0} = 1.5 \times 10^3$ km s^{-1} to estimate periods of oscillation.

3. Kink mode

Eq. (8) is solved for various lengths, densities and widths of loops. Ducted modes can be of *kink* or *sausage* type. Kink modes produce oscillations of the loop about its central axis, while the sausage modes give rise to loop motions resembling "heart beatings", with the plasma alternately moving away and towards the loop axis. See Fig. 4.

In the following, the results will be presented as contour plots of $v_n(\chi, \psi)$ in the flux coordinate system. The signature of a mode ducted by the loop will then be a normal velocity com-

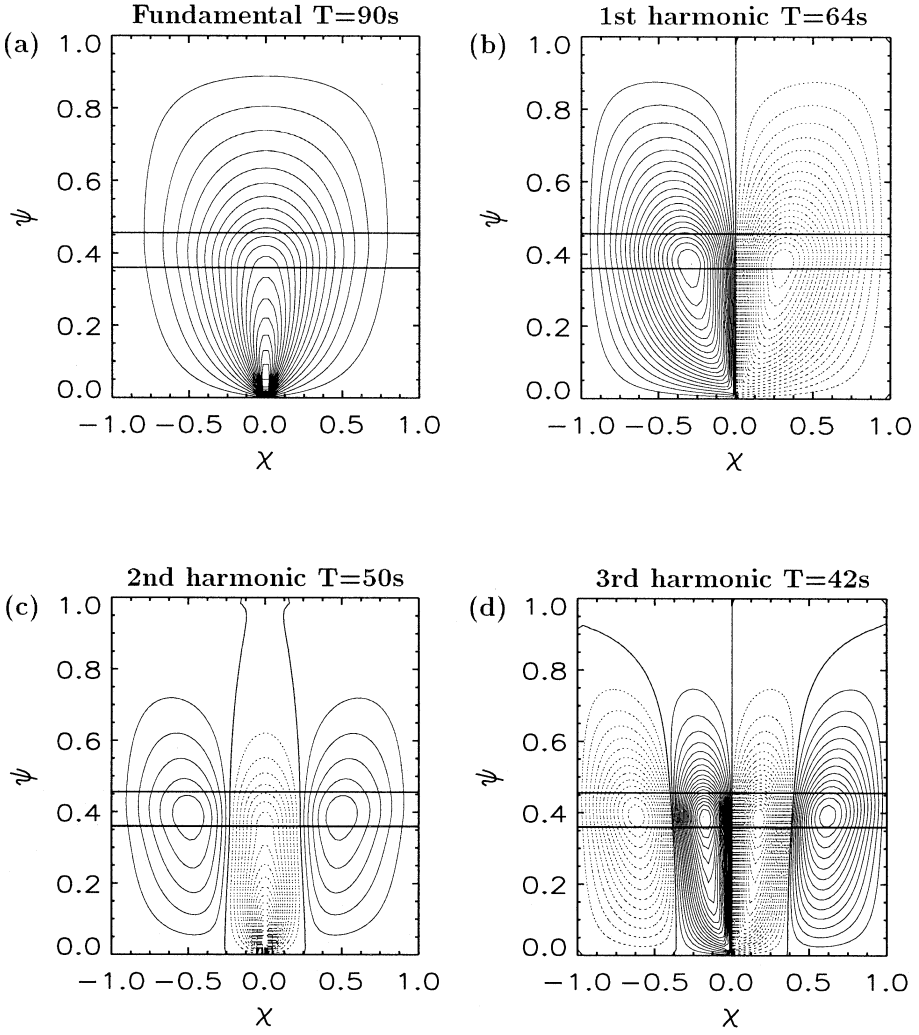

Fig. 5a–d. Kink mode - The effect of frequency of oscillation for a short loop, given by $0.36 \leq \psi \leq 0.46$, with moderate density enhancement (ρ = 5). Frequencies are measured in units of v_{A0}/L : $\omega_d \equiv \omega L/v_{A0}$. The motions v_n (in arbitrary units) in the flux coordinate system are displayed as contour plots for the four lowest frequency modes, with **a** ω_d=6.99 the lowest frequency mode, **b** ω_d =9.82, **c** ω_d =12.29, and **d** ω_d = 14.88 the third harmonic. The thin solid and dashed lines show contours of constant positive and negative velocity respectively. The two thick horizontal solid lines show the position of the dense loop. Note the odd modes (cases **b** and **d**) are efficient waveguides with v_n centred in the loop. The even modes (cases **a** and **c**) show increasing velocity outside the loop, suggesting leakage. In **c** we see the wave is trapped at $(\pm 0.5, 0.4)$ whilst the velocity peak at $(0, 0)$ has leaked from the loop. Even modes are more leaky than odd modes. Estimated periods $T\left(= 2\pi/\omega\right)$ of oscillation are given above each figure, taking $L = 1.5 \times 10^5$ km and $v_{A0} = 1.5 \times 10^3$ km s^{-1}

ponent that is maximum in the loop region and rapidly decays to zero outside the loop. Wave leakage from the loop is shown by large oscillatory amplitudes, comparable to the velocity in the loop, occurring outside the loop.

3.1. Effect of frequency

We start by looking at how wave leakage is influenced by the mode frequency. As with the finite slab or cylinder (Roberts et al. 1984), the line-tied loop has discrete modes because not all values of the wavelength along the loop are allowed. Kink modes present two types of geometry, either *even* or *odd* about the loop summit, characterised by a maximum or vanishing v_n at the top of the loop. When ordered by increasing frequency, kink modes are alternately even and odd, the fundamental mode being even, the first harmonic odd, and so on. The geometry of the kink mode is of importance in the ducting of perturbations. To show this we select a loop with conditions appropriate for leakage: a short loop with a moderate density enhancement (ρ = 5). Such conditions tend to reduce the ducting of the fast mode.

The velocity v_n of odd modes (zero velocity at the summit of the loop), shown in Figs. 5b and 5d, displays high values inside the loop with a rapid decrease in the surrounding corona, similar to what is found in the slab geometry. The wave energy is thus clearly ducted by the high-density loop. The results for the even modes (derivative of velocity zero at the top of the loop) are significantly different. Figs. 5a and 5c show high velocity amplitudes in the loop, although a dramatic increase in velocity outside the loop indicates the large leakage associated with these modes. In particular, for the second harmonic (Fig. 5c) we see the wave is clearly ducted at $(\pm 0.5, 0.4)$ whilst the velocity at $(0, 0)$ has leaked from the loop. These results are repeated for higher harmonics although odd modes become more leaky at higher frequencies. Ultimately, for very high frequencies, the ducted mode is destroyed. The modes described above correspond to the principal kink mode, i.e., with no change in the sign of v_n across the loop. Overtones of this mode have not been considered as they possess very high frequencies and are therefore less likely to be excited.

3.2. Length of loop

To examine the effect of the length of the loop on the trapping of waves by a density enhancement we consider ρ = 4 and the third

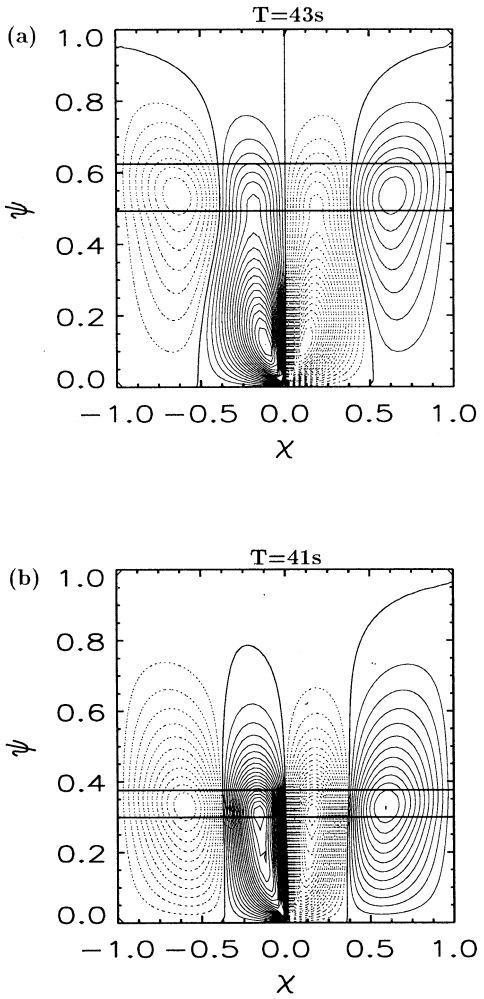

Fig. 6a and b. Kink mode - The effect of the length of the loop for density enhancement ρ = 4. A flux coordinate contour plot of the normal velocity component v_n for the third harmonic and **a** a short loop given by $0.49 \leq \psi \leq 0.62$ with frequency ω_d = 15.31, **b** a long loop given by $0.30 \leq \psi \leq 0.39$ with ω_d = 12.15. The ratio of the total length of the loop to the distance between its footpoints is 1.22 in **a** and 1.42 in **b**. The longer the loop, the smaller the effect of curvature and the more efficient the wave trapping. Periods T of oscillation for the two cases are given above the figures

harmonic. Such a small density enhancement makes the loop a poor waveguide for the kink mode, as can be appreciated from Fig. 6a in which a short loop has been considered. In Fig. 6a we see wave ducting occurring at $(\pm 0.7, 0.55)$, whilst the two central peaks at $(\pm 0.25, 0.1)$ have clearly leaked from the dense loop. However, for a long loop (Fig. 6b) the mode is ducted. A clear peak in v_n exists in the loop, flanked by two regions of strong velocity decrease suggesting leakage is minimal. These results show that long loops are a more efficient wave trap than short loops.

3.3. Density of loop

We now examine the effect of changing the gas density ratio on wave leakage. We consider the third harmonic in a short loop, for which curvature effects should be most pronounced. The results are illustrated in Fig. 7. For a density enhancement of ρ =5 (Fig. 7a) the mode can be considered to be effectively ducted by the loop, with a clear peak in v_n in the loop and an evanescent velocity outside. Decreasing the gas density ratio to 4.25 (Fig. 7b) shows the two velocity peaks located at $(\pm 0.5, 0.3)$ have leaked from the loop and the leakage is much larger than in Fig. 7a. Decreasing the density enhancement further to 4.09 (Fig. 7c) shows the two central velocity peaks in the loop becoming leaky. Indeed for ρ = 4.05 (Fig. 7d) we see only a small velocity in the loop with a much larger leakage velocity outside. In fact, decreasing the density ratio further (not shown) results in the destruction of the mode. These results show that leakage is more significant in low density enhancements (weak slabs) and decreases for high gas density ratios (strong slabs).

As one can see from the results described in Sect. 3.1 the first and third harmonics are more strongly guided than the second harmonic. The fundamental mode is more leaky than the second harmonic and longer loops or higher densities are needed to achieve efficient guiding of the oscillations.

3.4. Width of loop

To finish our study of the kink mode, we look at how the width of the loop changes the nature of the ducted wave. We consider a loop and fix its lower field line (the solid line in Fig. 8a) but vary the upper field line of the loop (to one of the dashed lines in Fig. 8a). Again, adverse conditions for the guiding of waves are considered. Results are obtained for a density enhancement of 6 and the second harmonic. For the narrowest loop (Fig. 8b) a ducted wave is observed at $(\pm 0.5, 0.4)$, although leakage is large, especially the central peak. Increasing the width (Fig. 8b) shows the velocity in the loop is much more pronounced although the central velocity peak is still very leaky. However, for the widest loop wave ducting is much more efficient with higher velocities inside the loop region, including the central peak, although leakage is still observed. Increasing the width (Figs. 8c, d), results in a decrease in leakage. Therefore, wide coronal loops are more effective wave traps than narrow ones.

4. Sausage mode

The results for the kink and sausage modes turn out to be similar; accordingly we only summarise the main results of the sausage mode.

Whereas in Sect. 3 pure kink waves were found, the sausage mode exists only in a hybrid form: the loops are found to oscillate symmetrically at the top, where the loop is widest, but the lower, narrower, parts oscillate asymmetrically.

In agreement with the infinite slab or cylinder cases (Edwin & Roberts 1982, 1983), the sausage mode exists only for wavenumbers above a critical value; in the infinite slab case,

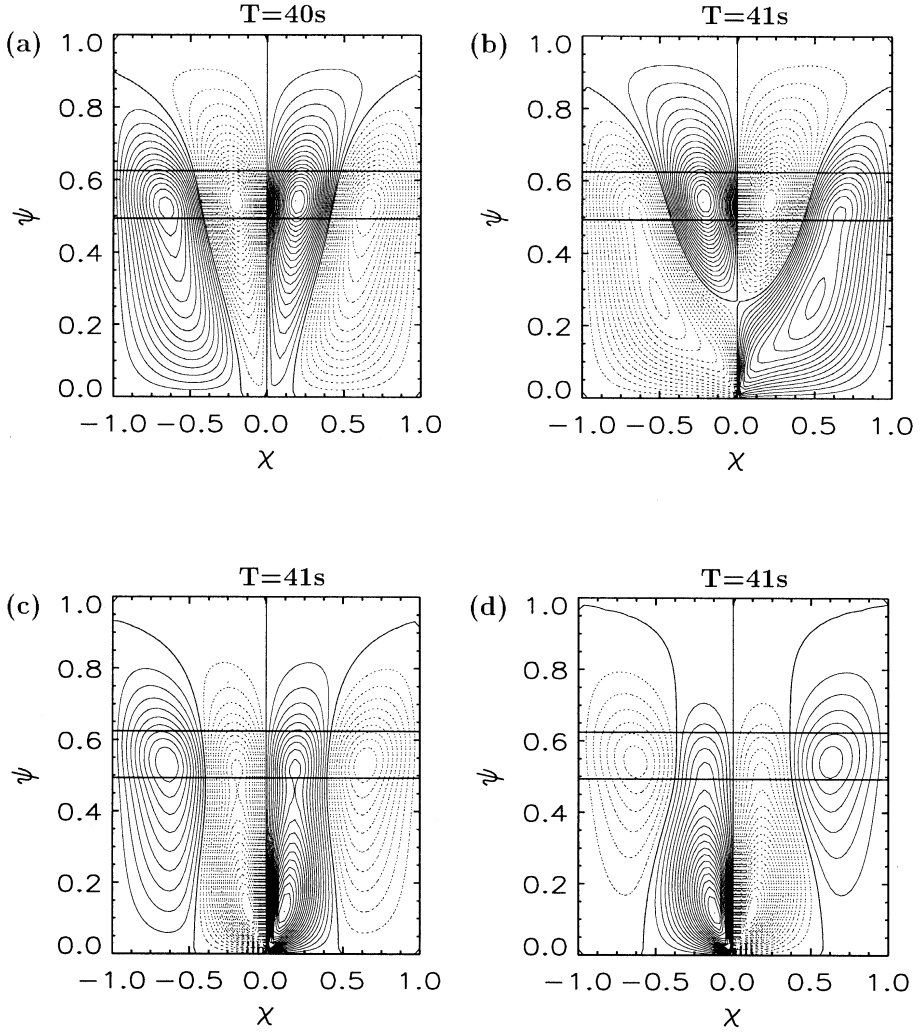

Fig. 7a–d. Kink mode - The effect of changing the density enhancement of the loop $0.49 \leq \psi \leq 0.62$ for the third harmonic. Contour plots of v_n are shown for **a** ρ = 5.0, ω_d = 15.76, **b** ρ = 4.25, ω_d = 15.35, **c** ρ = 4.09, ω_d = 15.37 and **d** ρ = 4.05, ω_d = 15.37. Weak slabs with low gas density (cases **b**, **c** and **d**) are much more leaky than strong, high gas density slabs (case **a**). Periods of oscillation are given above each figure

this is the k^{crit} of Eq. (1). We refer to the minimum frequency sausage mode as the *critical* mode.

Sausage modes tend to be more leaky than kink modes (sometimes even in long loops or for relatively large values of the density ratio ρ), although the two modes have some features in common. In a similar manner to kink modes, sausage modes have a velocity v_n that is alternately even and odd about the loop summit and, as found in Sect. 3.1, the odd modes appear to be more confined than the even modes. Moreover, increasing the frequency tends to produce an increase in leakage. The critical mode produces similar results to the slab geometry and in the loops considered is ducted with minimal leakage. The leakage in other modes depends on their frequency and on whether the normal velocity component is even or odd about the loop summit. As for the kink mode, short loops are more leaky than long loops. Also the higher the density ratio, the smaller the leakage from the loop. This implies there is a greater energy loss associated with weak loops. We find wave ducting is more efficient in wide loops. This has important consequences since in the slab geometry it is possible to use arbitrarily small values of the slab width $2a$ to obtain short periods (see Eq. [2]). However, in a curved geometry this is not possible since leakage increases and ultimately the mode is destroyed.

5. Discussion

Our numerical investigation into ducted waves in curved coronal loops has shown, as in curved waveguides, that leaky waves arise in curved structures. These waves will propagate away from the density enhancement and may be responsible for some of the reported coronal oscillations.

The critical sausage mode exhibits minimal leakage in all the loops considered. Using typical coronal values of 2×10^5 km for the distance $2l$ between loop footpoints and an Alfvén speed of $v_{A0} = 1.5 \times 10^3$ km s^{-1} within a loop, we find sausage mode periods of a few seconds, in agreement with the straight slab and cylinder work of Roberts et al. (1983, 1984). Hence the abundantly reported short period oscillations (see Introduction) may indeed be due to the critical sausage mode and its low harmonics. Higher sausage harmonics are not likely to be observed in coronal loops because of the large leakage. We find, using typical coronal values for L and v_{A0}, periods are of the order of a few seconds (Roberts et al. 1983, 1984). The fundamental

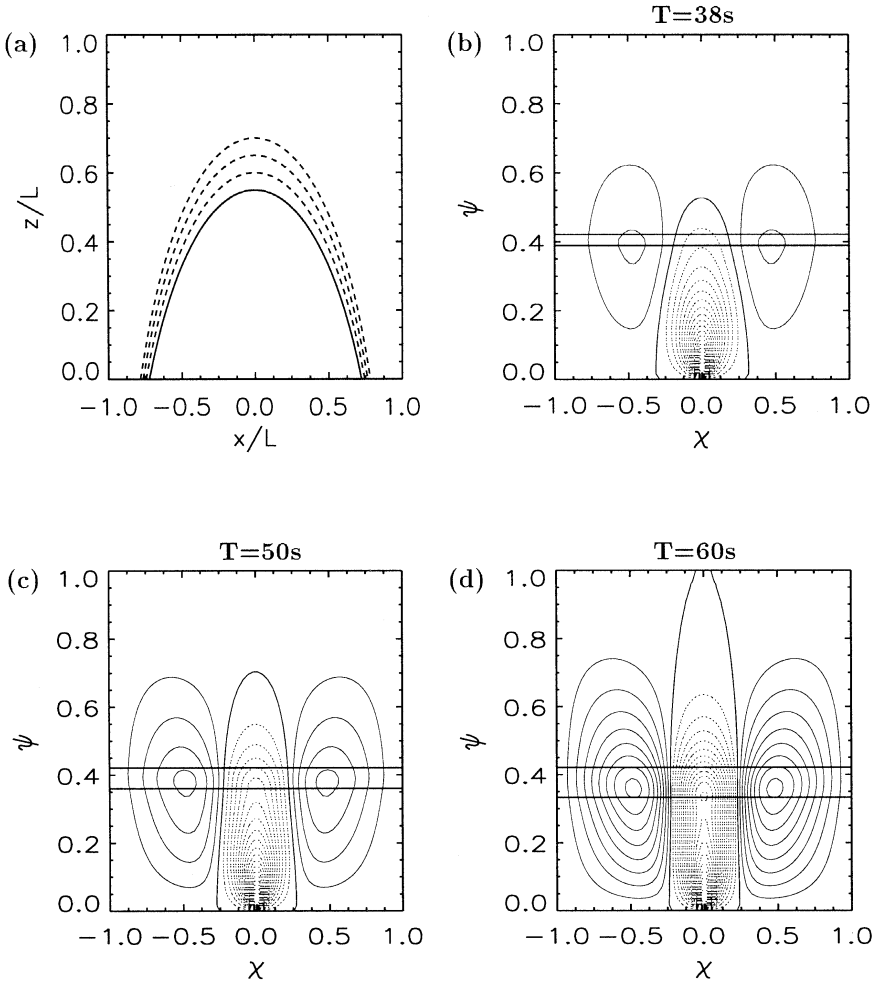

Fig. 8a–d. Kink mode - The effect of the width of the loop on leakage of the second harmonic in a loop with a density enhancement ρ = 6. **a** The three loops considered, shown in (x, z) coordinates, have their boundaries on a fixed field line (lower solid line of loop, ψ = 0.42) and one of the three dashed lines. Contour plots of v_n in flux coordinates are shown for **b** a narrow loop, ψ = 0.39, ω_d = 14.11 (T=38 s), **c** an intermediate width loop, ψ = 0.36, ω_d = 12.39 (T=50 s) and **d** a wide loop, ψ = 0.33, ω_d = 10.27 (T=60 s). Wave guiding is much more efficient in wide loops

kink mode is found to have periods in the range 40 to 60 seconds, also in agreement with the analytical work of Roberts et al. For shorter loops (e.g. 2×10^4 km) periods are between 4 and 6 seconds, typical of observed periods. Since the kink mode is less prone to leakage, higher harmonics may account for some of the observations. However, it is likely that some of the reported periods are due not to oscillations specifically within a loop but to the waves that leak from it.

The extent of the leakage depends upon the length, width and density enhancement of the loop, as well as the mode and frequency of oscillation. Increasing the length, width and gas density ratio reduces leakage, whilst higher harmonics result in an increase in energy leakage. In addition, even harmonics are less confined than odd harmonics and the sausage mode is more affected by the loop curvature than the kink mode, and is thus more leaky.

We may offer some physical explanations of these results. Firstly, it is worth recalling the results of Murawski & Roberts (1993) who considered ducted waves in a smoothed slab geometry embedded in a uniform field. They found for the sausage mode that waves with low frequency or in wide slabs leak less energy. Additionally, the energy leakage is lower for stronger slabs (higher density ratio). Also, the kink wave was much more robust than the sausage mode and consequently the sausage mode was more prone to leakage. The energy leakage in a spatially smooth density profile for the kink mode was negligibly small, even for weak slabs. The effectiveness of wave guidance depends upon the Alfvén speed profile — the smoother the profile, the higher the leakage. These results for a straight slab in a uniform field are in good agreement with the results in the curved structure presented here.

For long loops the geometry is less significant and the situation is similar to the slab case. Hence the leakage is less from these loops. Long loops have a length which is much greater than the horizontal distance between the two footpoints. In such loops the effect of curvature is small. In short loops, with length comparable to the horizontal distance between footpoints, curvature is a much more important factor. Short loops have greater curvature and so, by analogy with waveguide theory (Gloge 1972), the larger the effect of curvature the greater the leakage. Hence the smaller the loop, the greater the energy loss.

Loops with high gas density ratio (i.e. strong slabs) act as effective waveguides and leakage from these loops is small. Low density enhancements (i.e. weak slabs) are inefficient wave traps and waves are able to leak more readily. Therefore for high density active region and flare loops ($\rho > 10$) we may expect

leakage to be negligible. For lower density active region loops, say $\rho < 10$, wave ducting will be more inefficient.

With high modes of oscillation the waves 'feel' the curvature more than lower modes. Hence higher frequencies lead to increased leakage. Therefore it is not possible to consider an arbitrarily high harmonic to explain observations. This is a familiar result from waveguide theory where higher harmonics leak more strongly due to the angle of incidence of the wave on the boundary (e.g. Young 1986). In waveguide theory there is a critical mode above which ducted waves will not propagate. This has been considered in curved waveguides by Gloge (1972) and agrees with our numerical results. In addition, odd modes, with a node at the summit of the loop, have a wavelength which minimises the effect of curvature, thus reducing the leakage.

The sausage mode has its kinetic energy density located near the loop edges, whereas for the kink mode the energy is located in the centre. Therefore the kink mode is much more robust to curvature and waves are more confined. In addition, the sausage mode has a nodal line (zero v_n) in the centre of the loop. Hence curvature effects are stronger since part of the curve is stationary. For the kink mode the entire loop oscillates so curvature is not as strongly felt. Also, the velocity is greater at the interface for the sausage mode and (since energy loss is proportional to velocity squared) so the sausage mode will tend to lose more energy.

A similar argument applies for the results concerning the width of the loop. Wide loops have a smaller velocity at the loop interface and thus are less leaky. Narrow loops emphasise the curvature, which increases the leakage. The sausage mode was found to guide waves only for sufficiently large loop widths, which puts a lower bound on the period of this mode.

The hybrid nature of the sausage mode can be explained by the non-constant width of the curved loop. The loops considered have a maximum width at the summit of the loop. From the slab case (Roberts et al. 1983) the sausage mode occurs only above a threshold (Eq. [1]). Hence for a fixed mode (i.e. fixed k) this condition may be satisfied where the loop is wide, but not in the narrow parts of the loop. Where Eq. (1) is satisfied the loop will oscillate symmetrically, whereas asymmetric oscillations will be observed elsewhere.

Finally, it is worth mentioning that photospheric line-tying of field lines has no effect on the ducting properties of loops and only gives rise to discrete modes (as opposed to the continuous dependence of ω on k in the case of an infinite slab; Edwin & Roberts 1982). Therefore, the fast mode leakage in the present geometry must be ascribed solely to the curvature of the loop and not to its length.

Acknowledgements. J.M. Smith wishes to thank the United Kingdom Particle Physics and Astrophysics Research Council (PPARC) and the United Kingdom Engineering and Physical Sciences Research Council (EPSRC) for financial support and also additional support from the University of St Andrews (ERASMUS Grant 95-UK-3047/13) and NATO (under Grant CRG 901002) for his visit to Palma, where part of this work was undertaken. R. Oliver acknowledges support from the Spanish Ministery of Science and Education (Grant PB93-0420). J.M. Smith is grateful to K. Murawski and C. Mundie for constructive discussions and to J.L. Ballester for kind hospitality during his stay in Palma.

References

Acton, L. et al. 1992, Sci. 258, 618
Aschwanden, M.J. 1987, Sol. Phys. 111, 113
Aschwanden, M.J. 1994, Lecture Notes in Physics 444, Springer-Verlag, Heidelberg, pg. 13
Bray, R.J., Cram, L.E., Durrant, C.J., Loughhead, R.E. 1991, Plasma Loops in the Solar Corona, CUP, Cambridge
Čadež, V.M., Okretič, V.K. 1989, J. Plasma Phys. 41, 23
Cally, P.S. 1986, Sol. Phys. 103, 277
Cheng, C.-C. 1980, ApJ 238, 743
Davila, J.M. 1985, ApJ 291, 328
Doschek, G.A., Strong, K.T., Tsuneta, S. 1995, ApJ 440, 370
Edwin, P.M. 1984, PhD Thesis, University of St Andrews, Scotland
Edwin, P.M., Roberts, B. 1982, Sol. Phys. 76, 239
Edwin, P.M., Roberts, B. 1983, Sol. Phys. 88, 179
Foukal, P.V. 1975, Sol. Phys. 43, 327
Gloge, D. 1972, Applied Optics 11, 2506
Golub, L. 1991, in P. Ulmschneider and E.R. Priest (eds), Mechanisms of Chromospheric and Coronal Heating, Springer-Verlag, Heidelberg, pg. 115
Koutchmy, S. 1981, Space Sci. Rev. 11, 375
Meerson, B.I., Sasorov, P.V., Stepanov, A.V. 1978, Sol. Phys. 58, 165
Murawski, K., Roberts, B. 1993, Sol. Phys. 119, 399
Oliver, R., Ballester, J.L., Hood, A.W., Priest, E.R. 1993, A&A 273, 647
Oliver, R., Hood, A.W., Priest, E.R. 1996, ApJ 461, 424
Pasachoff, J.M., Ladd, E.F. 1987, Sol. Phys. 109, 365
Pasachoff, J.M., Landman, D.A. 1984, Sol. Phys. 90, 325
Pick, M., Trottet, G., MacQueen, R.M. 1979, Sol. Phys. 63, 369
Roberts, B., Edwin, P.M., Benz, A.O. 1983, Nature 305, 688
Roberts, B., Edwin, P.M., Benz, A.O. 1984, ApJ 279, 857
Roberts, B., Webb, A.R. 1979, Sol. Phys. 64, 77
Shibata, K. et al. 1992, Publ. Astron. Soc. Japan 44, L173
Snyder, A.W., Love, J.D. 1983, Optical Waveguide Theory, Chapman & Hall, London, pg. 495
Spruit, H.C. 1982, Sol. Phys. 75, 3
Stewart, R.T. 1976, Sol. Phys. 50, 437
Trottet, G., Pick, M., Heyvaerts, J. 1979, A&A 79, 164
Trottet, G., Kerdraon, A., Benz, A.O., Treumann, R. 1981, A&A 93, 129
Tsubaki, T. 1988, in R.C. Altrock (ed), Solar and Stellar Coronal Structures and Dynamics, NSO, Sunspot NM, pg. 140
Tsuneta, S. 1996, ApJ 456, 840
Van der Linden, R.A.M., Hood, A.W., Goedbloed, J.P. 1994, Sol. Phys. 154, 69
Wiehl, H.J., Benz, A.O., Aschwanden, M.J. 1985, Sol. Phys. 95, 167
Wilson, P.R. 1981, ApJ 251, 756
Young, M. 1986, Optics and Lasers (3 ed.), Springer-Verlag, Heidelberg, pg. 212
Zhao, R-Y., Jun, S-Z., Fu, Q-J, Li, X-Q. 1990, Sol. Phys. 130, 151
Zodi, A.M., Kaufmann, P. 1984, Sol. Phys. 92, 283

This article was processed by the author using Springer-Verlag LaTeX A&A style file *L-AA* version 3.